

0.96 D had been incorporated. The ^1H NMR spectrum of **3a** differed from that reported for **3** only in that the singlet at δ 3.0 integrated for 1 H.

Gas-Phase Pyrolysis of 3a. The gas-phase pyrolysis of 0.2 mmol of **3a** in 2 mL of CCl_4 was run at 126 °C as described for **3**. Adduct **4a**, after purification by HPLC, contained 0.96 D by mass spectrometry. The ^1H NMR spectrum of **4a** was identical with that of **4** except that the signal at δ 3.6 integrated for 7 instead of 8 H and the two signals at δ 2.4 and 2.05 appeared as doublets of doublets instead of as doublets of triplets. The ^2H NMR of **4a** contained signals at δ 3.6 and 2.05 in a ratio of 15:1.

The pyrolysis of **3a** was repeated under identical conditions except that the pyrolysis tube was packed with Pyrex beads. Identical results were obtained.

Determination of the 1° Isotope Effects for the Conversion of 3 to 2. A known mixture of **3** and **3a** was pyrolyzed in the gas phase at 122 °C under previously described conditions. The effluent containing both **1** and **3** was trapped with DMAD. The deuterium contents of purified **4** and **6** were determined by mass spectrometry, and the isotope effect was calculated. The values obtained for four separate experiments were 1.92, 1.93, 2.0, and 1.82 (average 1.92 ± 0.07).

Preparation of 3b. D_2O (41 mL) was slowly added to a stirred suspension of 0.42 g (10.7 mmol) of potassium in 130 mL of HMPA at 0 °C under N_2 . After H_2 evolution ceased, 83 mmol of **1** in 10 mL of benzene was added, and the solution was stirred for 22 h at 50 °C. The

reaction mixture was cooled, quenched with 3 mL of DOAc, poured into H_2O , and extracted three times with hexane. The combined extracts were washed four times with H_2O and dried over MgSO_4 . The solvent was removed by rotary evaporation, and the product was dissolved in 15 mL of benzene. For complete incorporation of four deuteriums into **1**, the above product was resubmitted to the above conditions. Reisolation of the product yielded (40%) tetradeuterated **1**, which by mass spectrometry contained ~ 4.0 D.

Diene **1-d₄** was converted to a mixture of **3b** and **1-d₃** by sequential treatment with *n*-BuLi and HOAc as previously outlined. The mixture was separated as before by selective cycloaddition of **1-d₃** with DMAD. By mass spectrometry the deuterium content of **3b** was 3.0 D. The NMR spectrum of the trideuterated **4** formed was identical with that reported for **4** except that the two doublets of triplets centered at δ 2.4 and 2.05 collapsed to singlets integrating for 0.55 and 0.45 H and the singlet at δ 3.6 integrated for 6 rather than 8 H.

Gas-Phase Pyrolysis of 3b. The pyrolysis of **3b** was run at 121 °C as previously described. The adducts were trapped with DMAD and purified; mass spectrometry revealed that **4b** contained 3.0 D. Adduct **4b**: ^1H NMR (CCl_4) δ 3.6 (s, 6.75 H), 2.92 (s, 2 H), 2.05 (s, 0.25 H), 1.4-1.4 (m, 4 H), 0.5 (m, 2 H).

Acknowledgment is made to the donors of the Petroleum Research Fund, administered by the American Chemical Society, for support of this research.

Bis(histamino)cyclodextrin-Zn-Imidazole Complex as an Artificial Carbonic Anhydrase

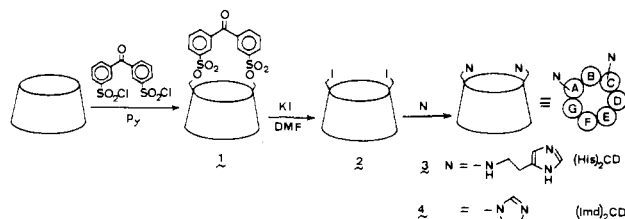
Iwao Tabushi* and Yasuhisa Kuroda

Contribution from Kyoto University, Department of Synthetic Chemistry, Yoshida, 606 Kyoto, Japan. Received September 28, 1983

Abstract: As a carbonic anhydrase model, bis(histamino)- β -cyclodextrin, $(\text{His})_2\text{CD}$, was prepared from benzophenone-3,3'-disulfonate capped cyclodextrin. The association constant of Zn^{2+} with $(\text{His})_2\text{CD}$ was determined to be $(4.5 \pm 2) \times 10^2 \text{ M}^{-1}$ at pH 7.5. The detailed kinetic analysis of the CO_2 hydration in imidazole buffer showed that $(\text{His})_2\text{CD} \cdot \text{Zn}^{2+} \cdot \text{Imd}$ -catalyzed CO_2 hydration where the observed catalytic constant was in the order of $10^3 \text{ M}^{-1} \text{ s}^{-1}$. Free $(\text{His})_2\text{CD}$, however, was rapidly converted to the corresponding carbamate, leading to a decrease in the catalyst concentration. Furthermore an unusual reaction of an indicator, *p*-nitrophenol, was observed only when $(\text{His})_2\text{CD} \cdot \text{Zn}^{2+} \cdot \text{Imd}$ was present. Competitive bicarbonate inhibition and protonation of the catalyst are also important for understanding both the sharp rate decrease during the course of the hydration and the negligible catalysis of bicarbonate dehydration.

Carbonic anhydrase is an enzyme widely distributed in plants, bacteria, and mammals, catalyzing the interconversion of CO_2 and HCO_3^- . This enzyme is well recognized as one of the typical Zn^{2+} -containing enzymes. Zn^{2+} is known to be bound to three imidazoles arranged in a nonplanar orientation. Because of the physiological importance of CO_2 hydration and the large rate acceleration, much attention has been focused on the interesting nature of this enzyme.¹ Although the structure,² spectroscopy,³

Scheme I



and kinetics⁴ of the enzyme have been investigated in detail, the mechanism of the catalysis has not yet been satisfactorily clarified. In spite of the particular attention to native carbonic anhydrase itself, there is only a limited number of studies available on artificial models actually catalyzing CO_2 hydration.⁵ Recent

(1) (a) Linkskog, S.; Henderson, L. C.; Kannan, K. K.; Lilljas, A.; Nyman, P. O.; Strandberg, B. *Enzymes*, 3rd Ed. 1971, 5, 587. (b) Coleman, J. E. In "Inorganic Biochemistry"; Eichorn, G. L., Ed.; Elsevier: New York, 1973; Vol. 1, p 488. (c) Buckingham, D. A. In "Biological Aspects of Inorganic Chemistry"; Addison, A. W., Cullen, W. R., Dolphin, D., James, B. R., Eds.; Wiley: New York, 1977; p 141. (d) Pocker, Y.; Sarkanen, S. *Adv. Enzymol.* 1978, 47, 149.

(2) (a) Lillja, A.; Kannan, K. K.; Bergsten, P. C.; Waara, I.; Fridborg, K. *Nature (London)* 1971, 235, 131. (b) Nostrand, B.; Waara, I.; Kannan, K. K. In "Isoenzyme. Molecular Structure"; Markert, C. L., Ed.; Academic Press: New York, 1975; p 575.

(3) (a) Linkskog, S. *Struct. Bonding (Berlin)* 1970, 8, 153. (b) Bertini, I.; Cantini, G.; Luchinat, C.; Scozzafava, A. *J. Am. Chem. Soc.* 1978, 100, 4874.

(4) (a) Pocker, Y.; Bjorkquist, D. W. *Biochemistry* 1977, 16, 5698. (b) Khalifah, R. G. *J. Biol. Chem.* 1971, 246, 2561. (c) Silverman, D. A.; Linkskog, S.; Tu, C. K.; Wynns, G. C. *J. Am. Chem. Soc.* 1979, 101, 6734. (d) Henkens, R. W.; Sturtevant, J. M. *Ibid.* 1968, 90, 2669.

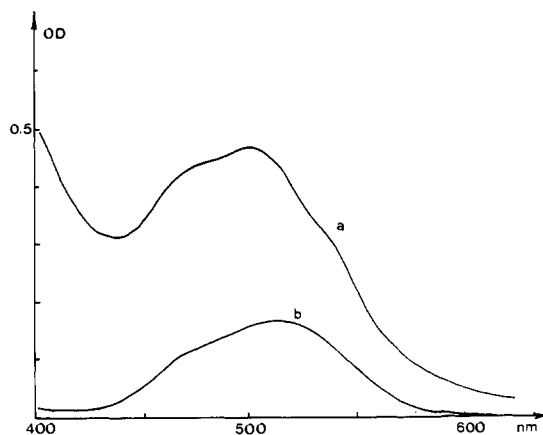


Figure 1. Visible absorption spectra of $(\text{His})_2\text{CD}\cdot\text{CO}_2^+$ at pH 7.5. (a) $[(\text{His})_2\text{CD}] = 2.5 \times 10^{-3} \text{ M}$, $[\text{CoCl}_2] = 2.5 \times 10^{-3} \text{ M}$; (b) $[\text{CoCl}_2] = 2.5 \times 10^{-3} \text{ M}$.

investigations on modified cyclodextrins as excellent artificial enzymes reveal the great advantage of "capping" for the regioselective modification of cyclodextrin.⁶ These successes have compelled us to apply the capping technique to the preparation of an artificial carbonic anhydrase to gain further insights into the CO_2 hydration mechanism.

Our proposed model, the bis(histamino)- β -cyclodextrin- Zn^{2+} -imidazole complex, showed reasonable catalytic activity as briefly reported.⁷ In this article, we report detailed mechanistic investigation of the carbonic anhydrase model. The present results show that the mechanism of the artificial enzyme-catalyzed hydration is much more complicated than that previously expected;⁷ i.e., (a) the present catalyst, $(\text{His})_2\text{CD}\cdot\text{Zn}^{2+}$. Imd, accelerates CO_2 hydration remarkably with a catalytic constant in the order of $10^3 \text{ s}^{-1} \text{ M}^{-1}$; (b) free $(\text{His})_2\text{CD}$ was rapidly converted to the corresponding carbamate, leading to a decrease in the catalyst concentration. This side reaction together with a pH drop and bicarbonate inhibition caused the decrease in the hydration rate. Furthermore, in this $(\text{His})_2\text{CD}\cdot\text{Zn}^{2+}$ catalysis, an unusual reaction of an indicator, *p*-nitrophenol, was observed. Although the catalytic activity of the present model is still considerably smaller than that of the native enzyme, the results described here may provide information for molecular design of a better carbonic anhydrase model.

Results and Discussion

Preparation of Cyclodextrin Catalyst. All catalysts used in the present study were prepared from benzophenone-3,3'-disulfonate-capped cyclodextrin (**1**)⁸ via diiodocyclodextrin (**2**) (Scheme I), which is a versatile intermediate for preparation of disubstituted cyclodextrins due to its high reactivity toward various types of nucleophiles under mild conditions.⁹ The purification of final products was easily achieved by a CM Sephadex ion-

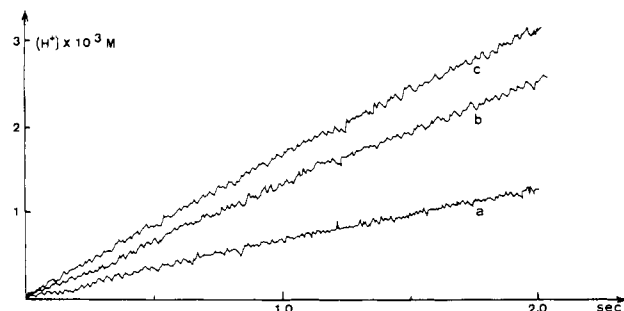


Figure 2. Typical reaction traces of CO_2 hydration at pH 7.0. (a) $[\text{Imd}] = 5 \times 10^{-2} \text{ M}$; (b) $[\text{Imd}] = 5 \times 10^{-2} \text{ M}$, $[\text{ZnCl}_2] = 5 \times 10^{-3} \text{ M}$; (c) $[\text{Imd}] = 5 \times 10^{-2} \text{ M}$; $[\text{ZnCl}_2] = 5 \times 10^{-3} \text{ M}$, $[(\text{Imd})_2\text{CD}] = 1 \times 10^{-3} \text{ M}$. In all reactions, neutral red was used as the indicator.

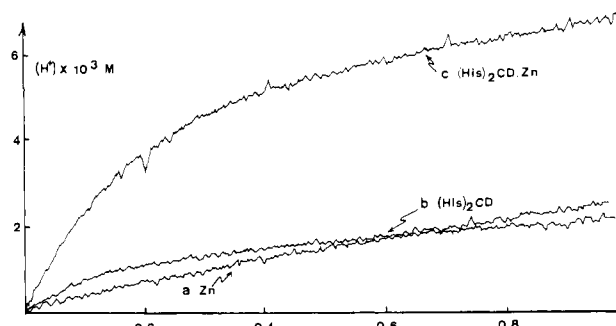


Figure 3. CO_2 hydration catalyzed by $(\text{His})_2\text{CD}$ at pH 7.5. (a) $[\text{Imd}] = 5 \times 10^{-2} \text{ M}$, $[\text{ZnCl}_2] = 5 \times 10^{-3} \text{ M}$; (b) $[\text{Imd}] = 5 \times 10^{-2} \text{ M}$, $[(\text{His})_2\text{CD}] = 1 \times 10^{-3} \text{ M}$; (c) $[\text{Imd}] = 5 \times 10^{-2} \text{ M}$, $[\text{ZnCl}_2] = 5 \times 10^{-3} \text{ M}$, $[(\text{His})_2\text{CD}] = 1 \times 10^{-3} \text{ M}$. Buffer factor = $(5.2 \pm 0.1) \times 10^{-2} \text{ M/OD}$, $(\Delta A/\Delta t)_{t=0} = 6.2 \times 10^{-1} \text{ OD/s}$. Neutral red was used as the indicator.

Table I. Rate Constants of CO_2 Hydration^a

catalyst ^b	buffer	$k_{\text{obsd}}, \text{s}^{-1}$	$k_{\text{cat}}, \text{s}^{-1} \text{ M}^{-1}$	indicator ^c
none	Imd	0.035 ± 0.002		PNP, NR
Zn	Imd	0.075 ± 0.01	8 ± 1^d	PNP, NR
$(\text{Imd})_2\text{CD}$	Imd	0.036 ± 0.002	$\sim 0^e$	PNP
$(\text{Imd})_2\text{CD}\cdot\text{Zn}$	Imd	0.10 ± 0.02	$24 \pm 10^{f,g}$	PNP
MeHis	Imd	0.034 ± 0.003	0	PNP
MeHis-Zn	Imd	0.077 ± 0.003	0	PNP
none	HEPES	0.038 ± 0.004		PNP
Zn	HEPES	0.047 ± 0.003	2 ± 2	PNP
$(\text{Imd})_2\text{CD}\cdot\text{Zn}$	HEPES	0.046 ± 0.002	0	PNP

^a $T = 25^\circ \text{C}$, pH 7.0, $[\text{buffer}] = 5 \times 10^{-2} \text{ M}$, $[\text{CO}_2] = 1.69 \times 10^{-2} \text{ M}$. ^b $[\text{ZnCl}_2] = 5 \times 10^{-3} \text{ M}$, $[\text{Imd}] = 5 \times 10^{-2} \text{ M}$. ^c PNP = *p*-nitrophenol, NR = neutral red. ^d $k_{\text{cat}} = (k_{\text{obsd}}^{\text{Zn}} - k_{\text{obsd}}^{\text{none}})/[\text{Zn}^{2+}]$. ^e $k_{\text{cat}} = (k_{\text{obsd}}^{\text{cat}} - k_{\text{obsd}}^{\text{none}})/[\text{Imd}]$. ^f $k_{\text{cat}} = (k_{\text{obsd}}^{\text{cat}} - k_{\text{obsd}}^{\text{Zn}})/[\text{Imd}]$. ^g Since the concentration of the catalyst is not corrected for the complexation of $(\text{Imd})_2\text{CD}$ with Zn^{2+} , the value of k_{cat} is a lower limit.

exchange column by applying a NH_4HCO_3 gradient, and pure products were obtained as free amines. Strongly basic histamines are better stored in the form of tetrahydrochlorides,¹⁰ because the free amine easily reacts with carbon dioxide to form carbamate. It was shown¹¹ that the present A,C isomer content was 82% (A,D 18%), but preliminary results showed that the catalytic activities for the CO_2 hydration of A,D isomers were very similar to the A,C isomers.

Metal Binding. The present carbonic anhydrase model, $(\text{His})_2\text{CD}$, binds Co^{2+} to develop the characteristic absorption (450–550 nm) at pH 7.5 as shown in Figure 1. Unsubstituted β -cyclodextrin does not show any absorption in the area. For similar concentration of *N*-methylethanolamine, however, no

(10) Excess HCl cleaves cyclodextrin appreciably.

(11) Information about the regioisomers of capped cyclodextrin is available in ref 8. Full description of the regiochemistry will appear soon in a full-length article.

(5) (a) Chaffe, E.; Dasgupta, T. P.; Harris, G. M. *J. Am. Chem. Soc.* **1973**, *95*, 4169. (b) Harrowfield, J. McB.; Norris, V.; Sargeson, A. M. *Ibid.* **1976**, *98*, 7282. (c) Huguet, J.; Brown, R. S. *Ibid.* **1980**, *102*, 7571. (d) Curtis, N. J.; Huguet, J.; Brown, R. S. *Ibid.* **1981**, *103*, 6953. (e) Brown, R. S.; Salmon, D.; Curtis, N. J.; Kusuma, S. *Ibid.* **1982**, *104*, 3188.

(6) For the capped-cyclodextrin family, see: (a) Tabushi, I.; Shimokawa, K.; Shimizu, N.; Shirakata, H.; Fujita, K. *J. Am. Chem. Soc.* **1976**, *98*, 7855. (b) Tabushi, I.; Yuan, L. C. *Ibid.* **1981**, *103*, 3574. (c) Tabushi, I.; Nabeshima, T.; Kitaguchi, H.; Yamamura, K. *Ibid.* **1982**, *104*, 2017. (d) Tabushi, I.; Yuan, L. C.; Fujita, K. *Tetrahedron Lett.* **1977**, 2503. (e) Tabushi, I. *Acc. Chem. Res.* **1982**, *15*, 66.

(7) Tabushi, I.; Kuroda, Y.; Mochizuki, A. *J. Am. Chem. Soc.* **1980**, *102*, 1152. Prof. Breslow kindly informed us about some carbamate formation. We are grateful for his constructive discussions.

(8) (a) Tabushi, I.; Kuroda, Y.; Yokota, K.; Yuan, L. C. *J. Am. Chem. Soc.* **1981**, *103*, 711. (b) Tabushi, I.; Yuan, L. C.; Shimokawa, K.; Yokota, K.; Mizutani, T.; Kuroda, Y. *Tetrahedron Lett.* **1981**, *22*, 2273.

(9) The use of **2** draws practical advantage from complete elimination of benzophenonedisulfonate in the course of purification of **2**. Benzophenonedisulfonate was sometimes difficult to remove from the product mixture obtained by the direct substitution on **1** with a nucleophile.

Table II. Rate Constants of CO₂ Hydration Catalyzed by (His)₂CD^a

Zn	buffer	pH ^d	k_{cat}^a , s ⁻¹ M ⁻¹	n recycl- ing ^b	k_{deact}^c , s ⁻¹ M ⁻¹
0	Imd	7.0	~0	1 ^c	340 ± 20
0	Imd	7.5	~0	1 ^c	800 ± 200
5 × 10 ⁻³	Imd	7.5	3100 ± 800	0	800 ± 200
			2600 ± 800	1	
			2400 ± 900	2	
2 × 10 ⁻³	Imd	7.8	3500 ± 800	0	920 ± 200
			3400 ± 700	1	
			3200 ± 900	2	
0	HEPES	7.0	~0	1 ^c	250 ± 100
5 × 10 ⁻³	HEPES	7.0	~0	1 ^c	270 ± 100

^a [(His)₂CD] = 1 × 10⁻³ M, *T* = 25 °C, [buffer] = 5 × 10⁻² M, neutral red was used as an indicator (540 nm) in all cases. ^b [H⁺ catalytically generated]/[(His)₂CD·Zn²⁺·Imd]. ^c Stoichiometric reaction was observed. ^d At completion of reactions, pH decrease of the solution was found to be less than 0.3 pH unit in all reactions.

remarkable absorption of Co²⁺ complex was observed in the region but weak shoulders at 520 and 650 nm were observed. When a large excess of imidazole ([Imd] = 5 × 10⁻² M, [CoCl₂] = 2.5 ± 10⁻³ M) was added, the corresponding complex showed an absorption at 507 nm. Preliminary results indicate that a group of p*K*_a = 7.5 participates the present coordination.¹² Therefore, imidazole-Co²⁺ complex is the most likely binding species of (His)₂CD. On the basis of the measurements for a series of (His)₂CD concentrations, the association constant of Co²⁺ with (His)₂CD was determined to be (2.4 ± 0.6) × 10² M⁻¹ and λ_{max} and ε corrected for the association were estimated as 503 nm and 40 M⁻¹ cm⁻¹, respectively.¹³ From the competitive binding¹⁴ of Zn²⁺ with Co²⁺, monitored by the (His)₂CD·CO²⁺ absorption decrease, the association constant of Zn²⁺ with (His)₂CD was estimated to be (4.5 ± 2) × 10² M⁻¹ at pH 7.5. Thus the present model, (His)₂CD, affords a reasonably strong binding site for Zn²⁺ in neutral pH region, in spite of the fact that (His)₂CD has only two imidazole groups.

Kinetic Studies. In the case of the Zn²⁺ complexes of (His)₂CD and (Imd)₂CD, the rate of the reaction followed by the indicator method¹⁵ fitted to eq 1 and from zero-order kinetics for the initial

$$\left(\frac{d[\text{H}^+]}{dt} \right)_{\text{initial}} = Q \left(\frac{d(\text{Abs})}{dt} \right)_{\text{initial}} = k_{\text{obsd}} [\text{CO}_2]_0$$

$$Q = \text{buffer factor} \quad (1)$$

stages of the reactions rate constants were obtained (Figure 2). The results are summarized in Table I. As suggested by Pocker et al.,^{4a} Zn²⁺ in imidazole buffer showed a small catalytic effect of $k_{\text{cat}} = 8 \pm 1 \text{ s}^{-1} \text{ M}^{-1}$. The Zn²⁺ complex of (Imd)₂CD showed the further acceleration of the CO₂ hydration where k_{cat} is 24 ± 10 s⁻¹ M⁻¹. It should be noted that both Zn²⁺ and imidazole buffer are essential for the catalytic activity of (Imd)₂CD and no appreciable catalysis was observed in the HEPES buffer (Table I). The kinetic aspect of (His)₂CD catalysis is quite different for Imd·Zn²⁺ or (Imd)₂CD·Zn²⁺ as is shown in Figure 3 and Table II. Proton generation at the initial stages of the reaction was very fast followed by the slower spontaneous CO₂ hydration (Figure 3c). It is important to note that moderate recycling of the catalyst, (His)₂CD·Zn²⁺·Imd, was observed within the initial fast portion of the kinetics. As shown in Figure 3b, (His)₂CD, in the absence of Zn²⁺, showed a simple nonrecycling burst reaction probably due to carbamate formation. These observations

(12) The preliminary results for (His)₂CD·Zn²⁺ show that the p*K*_a of imidazole determined by the NMR titration and by the kinetic behavior are appreciably different, being 6.5 ± 0.1 and 7.3 ± 0.1, respectively. These results suggest that the catalytically active group of the present catalyst is the water molecule coordinating to Zn²⁺. The detailed discussion will appear in near future.

(13) Estimation of ε for (His)₂CD·Co²⁺ complex was made by extrapolation to infinite concentration of (His)₂CD.

(14) Tabushi, I.; Fujiyoshi, M. *Tetrahedron Lett.* **1978**, 2157.

(15) Gibbons, B. H.; Edsall, J. T. *J. Biol. Chem.* **1963**, 238, 3502.

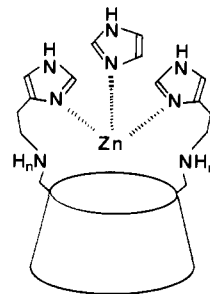
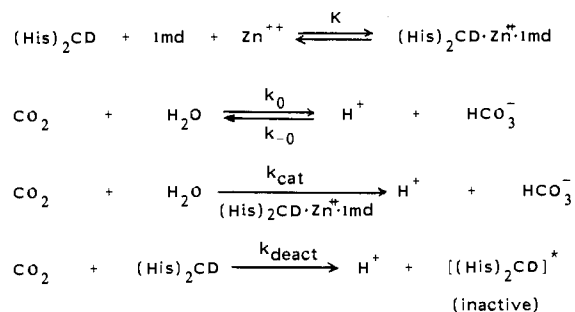


Figure 4. Active site of carbonic anhydrase model.

Scheme II

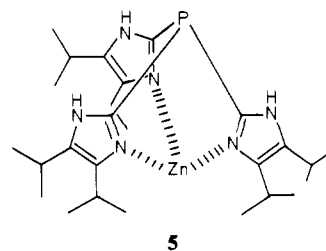


clearly demonstrate that (His)₂CD·Zn²⁺·Imd accelerates the catalytic CO₂ hydration, and at the same time, a competing irreversible deactivation reaction of free (His)₂CD takes place (Scheme II). The detailed analysis of the kinetics (see Experimental Section) reveals that, even after a stoichiometric amount of CO₂ (2 equiv of CO₂ per mol of catalyst) is hydrated, (His)₂CD·Zn²⁺·Imd still shows considerable catalytic activity (e.g., at pH 7.5 and 7.8; see Table II). The catalytic activity of (His)₂CD·Zn²⁺·Imd for CO₂ hydration gradually decreased,¹⁶ but recycling numbers of (His)₂CD·Zn²⁺·Imd, *r*, defined as

$$r = \frac{\text{total mol of CO}_2 \text{ catalytically hydrated}}{\text{mol of (His)}_2\text{CD}\cdot\text{Zn}^{2+}\cdot\text{Imd}}$$

are 8, 8, and 6 at pH 7.8, 7.5, and 7.0 (or 4, 4, and 3 per amino grouping), respectively.

At pH 6.5, however, the catalytic effect of (His)₂CD becomes very small even in the presence of Zn²⁺. The decrease is due to protonation-deactivation of the catalyst. As discussed for the HEPES buffer, an additional imidazole is essential to the catalysis. Therefore, a third coordinating imidazole molecule seems to be necessary to compose the present catalytic site (Figure 4). Recently, Brown et al. reported the rigid triimidazole Zn²⁺ complex **5**, which shows very effective catalysis in 80% ethanol without



any additional assisting grouping.^{5c,d} These results combined with

(16) The apparent decrease of the catalytic activity of (His)₂CD·Zn²⁺·Imd is considered to be due to the following effects on the basis of separate experiments: (a) the pH drop of the reaction system (protonation of imidazole), (b) the product (HCO₃⁻) inhibition (ligand substitution with Imd). In addition, unusually favorable formation of (His)₂CD carbamate in the presence of Zn²⁺ may also be expected. As to pH dependence of the complexation, 53% of total (His)₂CD forms the corresponding Co²⁺ complex at pH 7.5 but less than 15% at pH 6.5 on the basis of their visible spectra. Bicarbonate inhibition may be responsible for the loss of catalytic activity in the dehydration of bicarbonate.

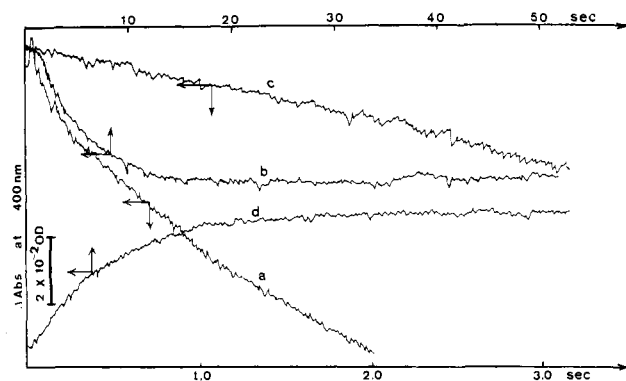


Figure 5. Reaction traces of CO_2 hydration and HCO_3^- dehydration in the imidazole buffer monitored by *p*-nitrophenolate absorption at 400 nm. (a) CO_2 hydration in the presence of $(\text{His})_2\text{CD}\cdot\text{Zn}^{2+}\cdot\text{Imd}$. (b) HCO_3^- dehydration in the presence of $(\text{His})_2\text{CD}\cdot\text{Zn}^{2+}\cdot\text{Imd}$. (c) CO_2 hydration in the presence of $\text{Zn}^{2+}\cdot\text{Imd}$. (d) HCO_3^- dehydration in the presence of $\text{Zn}^{2+}\cdot\text{Imd}$. The concentrations of components are as follows: $[(\text{His})_2\text{CD}] = 1 \times 10^{-3} \text{ M}$, $[\text{ZnCl}_2] = 5 \times 10^{-2} \text{ M}$, $[\text{CO}_2] = 1.69 \times 10^{-2} \text{ M}$, $[\text{HCO}_3^-] = 2 \times 10^{-2} \text{ M}$.

our present results show that a simple local model composed of three imidazoles coordinating to Zn^{2+} may be responsible for the catalytic effect of **5**, although the secondary amino grouping seems to promote the catalytic activity. The hydrophobic environment is another factor to enhance the CO_2 hydration activity, as is obvious from comparison of catalytic activities of $(\text{His})_2\text{CD}\cdot\text{Zn}^{2+}\cdot\text{Imd}$ with that of methylhistamine- Zn^{2+} -imidazole, the latter being least active.

Selection of Indicator. Since the indicator method was reported by Gibbons et al. in 1963, *p*-nitrophenol has been widely used as the indicator for the measurement of CO_2 hydration (and HCO_3^- dehydration) rates in the neutral pH region.^{4b,15} In the present rate measurements, however, we found that *p*-nitrophenol was not a suitable indicator in such a special case like ours.

As shown in Figure 5c,d, kinetic traces monitored at 400 nm are normal in CO_2 hydration and in HCO_3^- dehydration catalyzed by $\text{Zn}^{2+}\cdot\text{Imd}$; i.e., directions of absorbance changes in the hydration (Figure 5c) and the dehydration (Figure 5d) are in the opposite directions. In contrast to this normal behavior, the kinetics of the dehydration reaction catalyzed by $(\text{His})_2\text{CD}\cdot\text{Zn}^{2+}\cdot\text{Imd}$ shows an unusual behavior, where the "apparent increase" in proton concentration, measured by the absorbance change (Figure 5b), is in the opposite direction to the actual proton consumption. The present decrease of the absorbance seems to be due to the decrease in concentration of *p*-nitrophenolate ion in hydration as well as in the dehydration reaction, although the nature of the side reaction is not clear at the present stage.

We have concluded that neutral red behaved satisfactorily as an indicator in all the cases studied. Hydration rate constants are shown in Table II. Rate constants of other reactions were also measured with neutral red (Table I) and they were in good agreement with measurements by use of *p*-nitrophenol except $(\text{His})_2\text{CD}\cdot\text{Zn}^{2+}\cdot\text{Imd}$ catalysis.

Dehydration Reaction. Dehydration of bicarbonate was not appreciably accelerated by the present catalyst, $(\text{His})_2\text{CD}\cdot\text{Zn}^{2+}\cdot\text{Imd}$.¹⁷ The loss of activity is reasonably interpreted by the breakdown of the catalytically active species $(\text{His})_2\text{CD}\cdot\text{Zn}^{2+}\cdot\text{Imd}_2$ by bicarbonate coordination. The conclusion is supported by the bicarbonate inhibition observed in CO_2 hydration.¹⁶

Experimental Section

Commercially available reagents were used directly unless otherwise noted. The following spectroscopic instruments were used: Hitachi 215 grating IR spectrometer, JEOL PMX-60 and Varian HA-100 ^1H NMR spectrometer, Union SM-401 electronic spectrophotometer. Analytical HPLC was performed on Waters Associates ALP/GPC 204A by using a $\mu\text{Bondapak/CH}$ column with acetonitrile/ H_2O (5/1) as an eluant.

(17) This apparent inactivity was first observed by R. Breslow (private communication).

Detection of cyclodextrin derivatives on silica gel TLC (Merck Silica gel 60 F254) was achieved by the anisaldehyde method and/or the UV irradiation at 254 nm, the latter especially for capped cyclodextrins.¹⁸

Benzophenone-3,3'-disulfonate-Capped Cyclodextrin (1). To a solution of 40 g of carefully dried β -cyclodextrin (35 mmol) in 1 L of dry pyridine was added 13 g of freshly prepared benzophenone-3,3'-disulfonyl chloride¹⁹ (34 mmol) at room temperature. The reaction mixture was stirred for 30 min and pyridine was removed to dryness in vacuo at room temperature. The crude product was dissolved in 300 mL of water-EtOH (3/2) and the resultant solution was added dropwise into 4 L of acetonitrile/water (5/1) with vigorous stirring. The precipitate formed was filtered off, and the filtrate was evaporated to dryness in vacuo to afford 16.2 g of the crude product (42% yield). The product thus obtained was contaminated by a small amount (2.5%) of the double capped cyclodextrin^{8b} based on detailed HPLC analysis. Further purification of **1** was achieved by flash column chromatography on silica gel.²⁰ Thus, on a silica gel (Wako C-200) column (4 × 40 cm) pretreated with acetonitrile/water (5/1) was applied a solution of 2 g of **1** dissolved in 1.5 mL of DMF, and **1** was eluted with acetonitrile/water (5/1) by applying nitrogen pressure (ca. 0.1 kg/cm²). Appropriate fractions were combined, and after evaporation of solvent, 1.6 g of pure **1** was obtained, which exhibited a sharp single round spot of R_f 0.8 on silica gel TLC (*n*-PrOH- H_2O -AcOEt-Aqueous NH_3 , 5/3/2/1), detected by UV irradiation and anisaldehyde spray). Regioisomer ratio of this stage was 82% A,C + 18% A,D; ^1H NMR δ ($\text{Me}_2\text{SO}-d_6$) 3.3 (42 H, C₂, C₃, C₄, C₅, and C₆-H), 4.73 (7 H, C₁-H), 7.70, 7.87 (8 H, Ar H); IR (KBr) 2920, 1650, 1360, 1190, 1180, 1070, 1120 cm⁻¹.

Diiodo- β -cyclodextrin (2). To a solution of 7.2 g of **1** (5 mmol) in 300 mL of dry DMF was added 25 g of finely powdered potassium iodide (150 mmol). The solution was kept at 80 °C for 2 h with stirring. After the mixture cooled, insoluble materials were removed by filtration, and the solution was evaporated to dryness in vacuo at 30 °C. The residue was dissolved in 100 mL of water, and to the aqueous solution, 5 mL of tetrachloroethylene was added at 0 °C with vigorous stirring. The precipitate formed was collected and dried over P_2O_5 in vacuo to afford 6.2 g of **2** (92% yield). R_f value of **2** on TLC was very close to that of **1**, but **2** was practically nonilluminating toward UV irradiation and was detected only by the anisaldehyde method: ^{13}C NMR ($\text{Me}_2\text{SO}-d_6$); 102.03 (C₁), 81.39 (C₄), 72.11 (C₂, C₃, C₅), 59.87 (C₆ adjacent to OH), 9.50 (C₆ adjacent to I).

Bis(histamino)- β -cyclodextrin (3). To a solution of NaOEt freshly prepared from 170 mg of Na (7.4 mmol) and 15 mL of EtOH was added 680 mg of histamine dihydrochloride (3.7 mmol), and the solution was stirred at room temperature for 1 h under a nitrogen stream, the inlet and outlet of which were protected by KOH tubes. After removing insoluble material by filtration, the solution was concentrated to dryness. The residue was dissolved in 5 mL of degassed DMF and 500 mg of diiodo- β -cyclodextrin (0.37 mmol) was added into the resultant solution. The mixture was heated at 55 °C for 10 h under a nitrogen atmosphere. The solution was concentrated to dryness under vacuum, and 5 mL of EtOH was added to the residue with vigorous stirring. The insoluble material was collected by filtration, dissolved in 1 mL of water, and applied on a column of Sephadex CM-25 (NH_4^+ form, 2 × 60 cm). The column was washed with 100 mL of water and then eluted with a linear gradient of ammonium bicarbonate (total volume, 1 L; 0–0.5 M). The appropriate fractions (0.2–0.3 M NH_4HCO_3) were combined, and ammonium carbonate in the combined fractions was decomposed by evaporation under reduced pressure. The residue was finally treated with 0.5 N HCl, evaporated to dryness to afford 250 mg of A,C-bis(histamino)- β -cyclodextrin tetrahydrochloride (47% yield): TLC R_f 0.4 (silica gel, *n*-PrOH- H_2O -AcOEt-aqueous NH_3 , 5/3/2/1); ^1H NMR (D_2O) δ 9.50 (s, 2 H, C₂-H of imidazole), 8.25 (s, 2 H, C₅-H of imidazole), 6.00 (br s, 7 H, C₁-H of β -cyclodextrin), 5.0–4.0 (br m, 50 H, other protons). Anal. Calcd for $\text{C}_{52}\text{H}_{88}\text{O}_{33}\text{N}_6\text{Cl}_4\cdot 4\text{H}_2\text{O}$: C, 40.58; H, 6.29; N, 5.46; Cl, 9.21. Found: C, 40.21; H, 6.30; N, 5.11; Cl, 9.70.

General Procedure of Kinetic Measurements of CO_2 Hydration and HCO_3^- Dehydration. The rates of the hydration and the dehydration were determined by the indicator method reported by Gibbons and Edsall¹⁵ with modifications. Distilled water obtained by use of an automatic distillation apparatus (Toyo Co., GS-20N) was further purified by Gelman Sci. Inc. Water-I Laboratory Water System. The solution of CO_2 was prepared immediately before use by rapid bubbling of CO_2 gas through water at 25 °C for 20 min, and the concentration of CO_2 was determined to be $3.4 \times 10^{-2} \text{ M}$ by the $\text{Ba}(\text{OH})_2$ titration method.²¹ The

(18) Wiedenhof, N. *J. Chromatogr.* **1964**, *15*, 100–105.

(19) Work, J. L.; Herwch, J. E. *J. Polym. Sci., Polym. Chem. Ed.* **1968**, *6*, 2022.

(20) Still, W. C.; Kahn, M.; Mitra, A. *J. Org. Chem.* **1978**, *43*, 2923.

solution of bicarbonate (4.0×10^{-2} M) was prepared by dissolving 400 mg of KHCO_3 in 100 mL of carefully degassed water.

Preparation of a Catalyst Solution. A catalyst solution was prepared by dissolving an appropriate amount of a catalyst into 5 mL of a carefully degassed buffer solution containing 4×10^{-4} M of neutral red or 2×10^{-4} M of *p*-nitrophenol as an indicator. After the solution was diluted to 10 mL with degassed water or an aqueous ZnCl_2 solution (2×10^{-2} M), the pH of the solution was adjusted to a certain desired value by careful addition of 10 N HCl or 10 N NaOH.

Determination of Buffer Factor. For the determination of buffer factor, Q , 1.0 mL of the catalyst solution was mixed with the same volume of carefully degassed water, and the diluted solution was titrated with 0.01 N HCl. The absorbance of *p*-nitrophenolate absorption at 400 nm or that of neutral red absorption at 540 nm was recorded for every 5–10- μL addition of 0.1 N aqueous HCl. The absorbance of *p*-nitrophenolate absorption at 400 nm or that of neutral red absorption at 540 nm was recorded for every 5–10- μL addition of 0.1 N aqueous HCl. The absorbance changes observed (ΔA) were plotted against the total concentration of the added acid, $\Delta[\text{HA}]$, corrected for the volume change during the titration. The buffer factor, Q , was determined from the slope of the titration plot, $\Delta[\text{HA}]/\Delta A$.

Rate Measurements and Rate Analysis. All the kinetic measurements reported here were carried out with a Union RA-401 stopped-flow spectrometer thermostated at 25.0 °C. A solution of a catalyst and a CO_2 solution were driven together by 4 kg/cm² of nitrogen pressure and both solutions of equal volume were mixed within 2 ms. After mixing, the rapid absorbance change at 400 nm for *p*-nitrophenolate anion or at 540 nm for neutral red was stored in a Union RA-405 kinetic data processor and read out on a *X-Y* recorder after several traces were integrated. Usually, a reaction trace within 0.5–5 s was used for analysis. The absorbance change during the reaction was converted to the concentration change of proton (or bicarbonate) on multiplication by the buffer factor. Since the absorbance change observed for the reaction in

an imidazole or imidazole–zinc buffer solution showed excellent linearity with time at the early stages of the reaction, the first-order rate constants were directly obtained from the slopes of the linear portions according to eq 2. For all buffer–indicator systems, first-order dependency of the

$$k_{\text{obsd}} = \frac{(\Delta A / \Delta t)_{\text{initial}} Q}{[\text{CO}_2]_0 \text{ or } [\text{HCO}_3^-]_0} \quad (2)$$

values of $(dA/dt)_{\text{initial}}$ on the initial concentration of CO_2 ((1.7×10^{-2}) – (5.7×10^{-3}) M) was ascertained. Observed catalytic activity decreased during the course of the CO_2 hydration catalyzed by 3–zinc complex. Therefore, the rate constants were estimated by the following methods:

(1) The observed kinetic curves were corrected by subtracting the absorbance changes due to the spontaneous CO_2 hydration and the deactivation reaction of $(\text{His})_2\text{CD}$ under the corresponding buffer conditions from the observed overall absorbance change. The deactivation term was estimated from the rate constants of the reaction between free $(\text{His})_2\text{CD}$ and CO_2 and the actual concentration of free $(\text{His})_2\text{CD}$ calculated from $K_{\text{Zn}^{2+}}$.²²

(2) On the basis of the corrected kinetic curves thus obtained, the first recycling point was so defined that 1 mol of CO_2 per 1 equiv of histamino grouping was hydrated. It was calculated by using the observed absorbance change and the buffer factor.

(3) Pseudo-zero-order rate constants were obtained from slopes of the corrected kinetic curves at the initial and first or second “recycling” points.

(4) The zero-order rate constants were converted to first-order rate constants (k_1 , s⁻¹) by dividing by the concentration of CO_2 still remaining at each point.

(5) The catalytic constants (k_{cat} , M⁻¹ s⁻¹) were obtained from $k_1/[(\text{His})_2\text{CD} \cdot \text{Zn}^{2+} \cdot \text{Imd}]$, where the concentration of $(\text{His})_2\text{CD} \cdot \text{Zn}^{2+} \cdot \text{Imd}$ was calculated from $K_{\text{Zn}^{2+}}$.

Acknowledgment. We are grateful to Professor R. Breslow, Columbia University, for his thoughtful and helpful discussion on the catalysis.

Registry No. 1, 76700-69-1; 2, 76700-71-5; 3-4HCl, 90604-16-3; CO_2 , 124-38-9; β -cyclodextrin, 7585-39-9; benzophenone-3,3'-disulfonyl chloride, 17619-15-7; histamine dihydrochloride, 56-92-8; carbonic anhydrase, 9001-03-0.

(22) For example, in the case of Figure 3, the deactivation term was estimated from the reaction trace of Figure 3b and the concentration of free $(\text{His})_2\text{CD}$ calculated from $K_{\text{Zn}^{2+}}$.

Quantum Chemical Calculation of the Enzyme–Ligand Interaction Energy for Trypsin Inhibition by Benzamides

Gábor Náray-Szabó

Contribution from the CHINOIN Pharmaceutical and Chemical Works, H-1325 Budapest, Hungary. Received September 1, 1983

Abstract: Three-dimensional coordinates of the β -trypsin–benzamide complex were used to construct a quantum chemical model for the enzyme–inhibitor interaction. The model included all enzyme and benzamidinium ($\text{H}_4\text{N}_2\text{CC}_6\text{H}_4\text{X}^+$) atoms and two bound water molecules (W702 and W710) located near the binding site. Hydration was also treated by using a simple model of the first hydration sphere including four water molecules. The enzyme–inhibitor interaction energy was approximated as $\sum V_{\text{enz}}(r_a)q_a$, where the first term is the enzyme electrostatic potential at the position of atom *a* and the second term is the charge on this atom. The potential was calculated from bond fragments as proposed previously while net charges were obtained from CNDO/2 calculations. The hydration energy was calculated by the same expression, where V_{enz} was replaced by the potential of the four water molecules. It was found that the experimental Gibbs free energy of association, ΔG_{exptl} , depends linearly on the calculated interaction energy. A similar linear relationship was observed between the hydration energy and ΔG_{exptl} , indicating that the enzyme may be treated as a “supersolvent”. The “electrostatic lock” representing the active site of the enzyme is characterized, and the “key” (the charge pattern of the inhibitor) is found to fit into this lock. With use of this model as a guide, simple structure–activity relationships are derived which may be extended to other enzymes, like thrombin and plasmin.

In the search for potent bioactive compounds it is especially important to understand the nature of the interaction between biological macromolecules (enzymes, receptors) and small ligands

(inhibitors, drugs). A promising way is combination of the complete three-dimensional structure of the biomacromolecule–ligand complex with theoretical energy calculations.^{1–8} Owing